sustainability

MDPI

Article

Ecological Monitoring of Nuclear Test Sites over 20 Years Based on Remote Sensing Ecological Index: A Case Study of the Semipalatinsk Test Site

Aidana Sairike [1], Noriyuki Kawano [1,2], Vladisaya Bilyanova Vasileva [2] and Mianwei Chen [3,*]

[1] Graduate School of Humanities and Social Sciences, Hiroshima University, Higashi-Hiroshima 739-8529, Japan; d246383@hiroshima-u.ac.jp (A.S.)
[2] The Center for Peace, Hiroshima University, Hiroshima 730-0053, Japan
[3] Graduate School of Advanced Science and Engineering, Hiroshima University, Higashi-Hiroshima 739-8527, Japan
* Correspondence: d242883@hiroshima-u.ac.jp

Abstract

The Semipalatinsk Test Site (STS), one of the most heavily contaminated nuclear test sites globally, presents critical challenges for ecological monitoring and restoration due to long-term radioactive pollution and soil degradation. This study applied the Remote Sensing Ecological Index (RSEI) model to systematically evaluate the spatiotemporal changes in ecological quality at STS from 2003 to 2023. The RSEI model integrated multi-indicator data, including NDVI (Normalized Difference Vegetation Index), LST (Land Surface Temperature), WET (Wetness), and NDBSI (Normalized Difference Built-up and Soil Index), enabling a comprehensive assessment of ecological dynamics. Results demonstrated a significant improvement in ecological quality, with the RSEI increasing by 29.59% (from 0.345 in 2003 to 0.447 in 2023). PCA results indicated that ecological recovery was primarily influenced by surface temperature, vegetation cover, and soil moisture, with radioactive residues further hindering recovery in severely contaminated zones. The proportion of "Poor" areas declined from 14.99% to 0.61%, while "Moderate" and "Good" areas expanded to 55.76% and 8.87%, respectively. Peripheral regions showed faster recovery due to effective natural and management interventions, while core high-contamination zones (Sary-Uzen) exhibited slower recovery due to persistent radioactive residues. This study highlights the applicability of RSEI for assessing ecological recovery in nuclear test sites and emphasizes the need for targeted remediation strategies. These findings provide valuable insights for global ecological management of nuclear test sites, supporting sustainable restoration efforts.

Keywords: remote sensing; environmental assessment; Semipalatinsk test site; RSEI; principal component analysis

Check for updates

Academic Editors: Sheng Wang, Zhifeng Li and Jie Li

Received: 17 November 2025
Revised: 19 December 2025
Accepted: 23 December 2025
Published: 24 December 2025

Copyright: © 2025 by the authors. Licensee MDPI, Basel, Switzerland. This article is an open access article distributed under the terms and conditions of the Creative Commons Attribution (CC BY) license.

1. Introduction

The first nuclear test in human history, code-named "Trinity," was conducted on 16 July 1945, at the Alamogordo test site in New Mexico, USA [1]. During the Cold War, countries like the United States and the Soviet Union conducted numerous nuclear tests across atmospheric, underground, and underwater environments, contributing to the 2000 global tests recorded by 2023 [2,3]. The environmental impacts of nuclear testing are profound and devastating. The radioactive contamination generated by nuclear tests

has caused long-term damage to ecosystems, affecting soil, water sources, and air quality over extensive areas. This pollution poses severe health risks to wildlife and human communities, including increased rates of cancer and hereditary diseases [4–6]. International efforts to mitigate the health and environmental impacts of nuclear testing led to the signing of the Partial Test Ban Treaty (1963) and the Comprehensive Nuclear-Test-Ban Treaty (1996) [7,8]. Growing concerns over the environmental impacts of nuclear testing have underscored the importance of ecological monitoring and restoration in nuclear test sites [9]. Effective ecological monitoring is crucial for understanding the long-term impacts of nuclear testing, guiding restoration efforts, and supporting global environmental governance. Continuous monitoring ensures the sustainability of affected regions and provides valuable insights for addressing similar environmental challenges in the future.

Globally, several prominent nuclear test sites have become key areas for studying the long-term ecological impacts of nuclear testing [6]. However, the scientific quantification of ecological environments remains particularly important. At present, satellite remote sensing technology and Geographic Information Systems (GIS) have been widely applied in regional ecological environment assessments due to their advantages of large-scale monitoring, periodic updates, and real-time capabilities [10,11]. Nevertheless, traditional GIS approaches rely heavily on manual processing of large volumes of data, which can be overly cumbersome [12]. As an advanced cloud computing platform for remote sensing data, Google Earth Engine (GEE) provides global researchers with extensive satellite remote sensing data and powerful data processing tools [13]. Compared to traditional methods of acquiring and processing remote sensing data, the GEE platform offers advantages such as comprehensive data availability, rapid processing speeds, and operational simplicity [14]. Researchers no longer need to invest in expensive hardware or endure long processing times; GEE can quickly complete complex computational tasks on the cloud, ranging from simple image classification to intricate model simulations, all within minutes [15]. Furthermore, most current studies rely on single indicators to describe specific aspects of the ecological environment, such as using thermal infrared bands from remote sensing images to retrieve surface temperatures for urban heat island monitoring, or constructing various drought indices to assess regional drought conditions [16]. However, due to the complexity of ecosystems, single indicators often fail to comprehensively and effectively describe the ecological environment. Some scholars have adopted approaches such as the Analytic Hierarchy Process (AHP) and the Pressure-State-Response (PSR) model to integrate multiple indicators and construct composite indices for ecological environment assessment [17–19]. Nevertheless, these indices often face challenges such as difficulties in determining weights and high levels of subjective bias. Since Xu Hanqiu first proposed the use of the Remote Sensing Ecological Index (RSEI) to represent ecological environmental quality [20], the index has employed Principal Component Analysis (PCA) to couple four ecological indicators: greenness (NDVI), wetness (WET), dryness (NDBSI), and heat (LST) [21,22]. The RSEI is characterized by its simplicity in obtaining indicators and its avoidance of manual weight determination, and its reliability has been confirmed by multiple scholars to date [23–25].

The STS, established in 1947 in northeastern Kazakhstan, conducted 456 nuclear tests between 1949 and 1989, releasing vast radioactive materials that severely contaminated the soil, water, and atmosphere, causing long-term ecological damage and severe health issues for local populations. Strong anti-nuclear movements led to its official closure in 1991 following the Soviet Union's dissolution [26–28]. In 2008, Kazakhstan's National Nuclear Center conducted extensive environmental monitoring of the test site and its surrounding areas, delineating the boundaries between highly contaminated and less-contaminated zones, providing a scientific foundation for ecological restoration efforts [29]. In 2013,

Kazakhstan launched the "Semipalatinsk Nuclear Safety Zone" project, which adopted a zoning approach to separate highly contaminated areas from ecological restoration zones. This strategy aimed to prevent the further spread of radioactive contamination while enhancing monitoring and management of areas undergoing natural recovery [30,31]. The STS has become a symbol of the impacts of nuclear testing and the global anti-nuclear movement. In a region like Semipalatinsk, which has suffered from severe nuclear testing impacts, it is crucial to accurately assess the progress and current status of ecosystem recovery. Comprehensive evaluations of ecological quality not only provide valuable data and insights for scientists and policymakers but also serve as an effective monitoring and assessment framework for other regions worldwide facing similar challenges.

This study introduces, for the first time, the Remote Sensing Ecological Index (RSEI) for long-term ecological monitoring of the STS and its surrounding areas, marking the first application of RSEI to any nuclear test site. By integrating four key indicators—greenness (NDVI), wetness (WET), dryness (NDBSI), and heat (LST)—the study provides a comprehensive and precise assessment of ecological quality. Unlike traditional composite indices that rely on subjective weight assignment, RSEI employs principal component analysis (PCA) to derive objective weights from the data itself, significantly enhancing both the accuracy and reproducibility of ecological evaluations across large spatial and temporal scales. This is particularly important for a region like Semipalatinsk, which has been severely impacted by long-term nuclear testing, as it reveals various ecological changes caused by nuclear tests, including vegetation conditions, moisture status, bare soil dynamics, and surface temperature variations. The continuous time-series analysis provided by RSEI enables the observation of ecological recovery trends over time and the evaluation of the effectiveness of different ecological restoration strategies. Its efficiency in processing and analyzing large-scale remote sensing data makes it an ideal tool for assessing ecological quality in areas affected by nuclear tests. The proposed application of RSEI has played a critical role in the ecological monitoring of the STS and offers an effective method for monitoring and evaluating similarly damaged ecosystems worldwide. This innovative application not only provides valuable data for scientific research but also offers robust support for developing future environmental protection policies and management strategies.

2. Materials and Methods

2.1. Study Area

The STS is located in the Abai Region of the Republic of Kazakhstan, with Semey as the administrative center, established in June 2022, spanning longitudes 77.7° E to 79.1° E and latitudes 49.31° N to 50.93° N [32]. These 18,000 square kilometer test site overlaps with three modern regions of Kazakhstan: the Pavlodar Region, the Karaganda Region, and the Abai Region (formerly the Semipalatinsk Region). The study area for this research covers approximately 84,000 square kilometers (Figure 1).

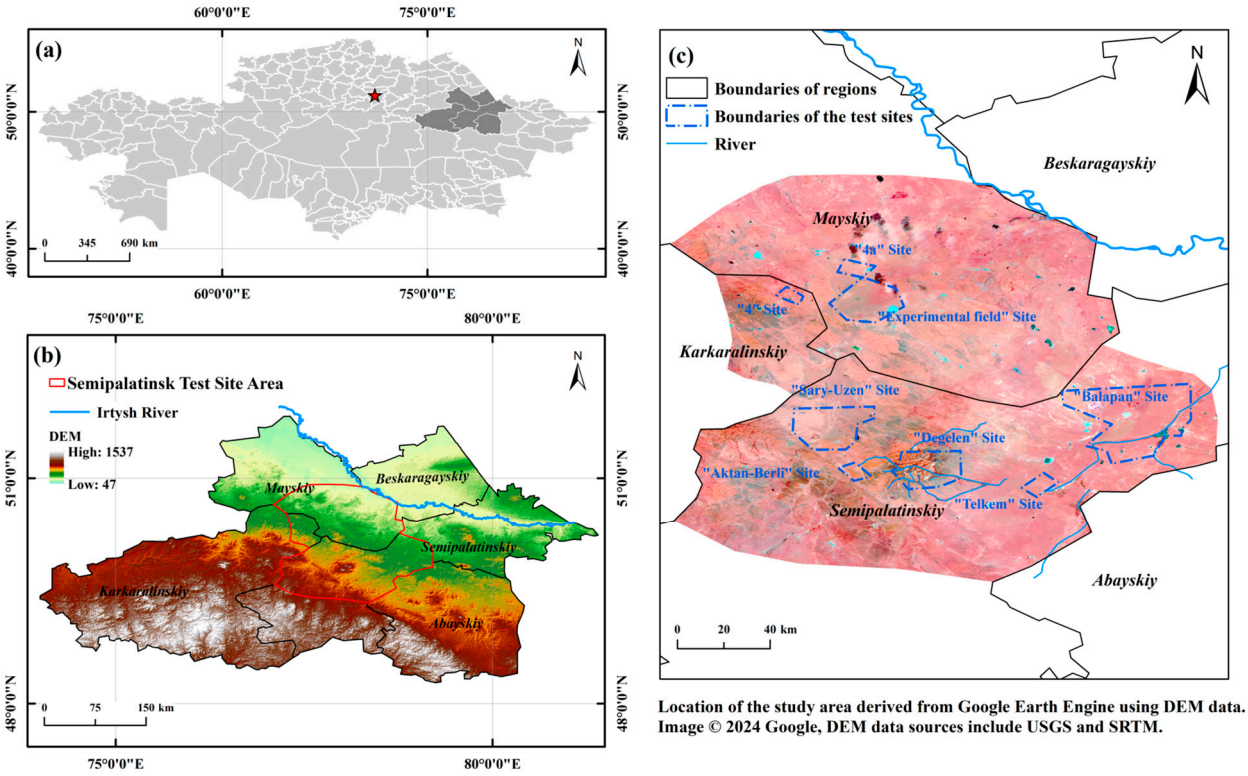


Figure 1. Schematic diagram of study area. (**a**) Geographic location of Semey within Kazakhstan. (**b**) Overview of the Semey region showing the overall study area, which includes the officially designated STS (core nuclear test zone) and the surrounding peripheral areas historically used for residential and logistical support. (**c**) False-color composite image derived from satellite data, illustrating the spatial extent of the core nuclear test zone and the distribution of major test sites and experimental fields. The color patterns represent spectral characteristics from the false-color composition rather than manually highlighted zones. The red star indicates the location of Astana, the capital of Kazakhstan.

2.2. Data Sources

This study utilizes Landsat remote sensing imagery from the Google Earth Engine (GEE) platform database, covering a 20-year period from 2003 to 2023. The data include Tier 1 surface reflectance products (SR) from Landsat 5 (TM) and Landsat 8 (OLI), with dataset identifiers LANDSAT/LT05/C02/T1_L2 and LANDSAT/LC08/C02/T1_L2, respectively, in GEE. These datasets have a spatial resolution of 30 m and a temporal resolution of 16 days. Due to the unavailability of early satellite data and imaging damage, this study selected data from 2003, 2008, 2013, 2018 and 2023 for analysis. The chosen data have undergone radiometric, atmospheric, and geometric corrections. Since vegetation is closely related to ecological quality and the RSEI uses vegetation greenness as a key indicator, the imagery must be from the vegetation growing season to ensure the accuracy of the retrieval results. Therefore, during GEE programming (using JavaScript), all Landsat images covering the study area were automatically retrieved based on predefined spatial, temporal, and quality criteria, including spatial coverage of the region of interest, acquisition dates between June 15 and August 15, and an overall cloud cover of less than 50%. The study area spatially spans nine Landsat scenes, which were mosaicked to ensure complete spatial coverage. Preprocessing procedures, including cloud and cloud-shadow removal using the QA_PIXEL band, pixel-wise mean compositing, spatial mosaicking, clipping to the study area, and water body masking based on the JRC Global Surface Water (GSW v1.3) dataset, were performed entirely on the GEE platform. These steps produced a single

annual composite image for each year and ensured the reliability and precision of the ecological indicators used for subsequent RSEI calculation.

2.3. Methods

In this study, the RSEI was calculated using Principal Component Analysis (PCA). The four key indicators, NDVI, WET, NDBSI, and LST, were first individually computed through respective models. To minimize errors, the data for these indicators were filtered to fall within the 5%~95% confidence interval and subsequently normalized. The normalized data were then synthesized into a single composite dataset through band stacking. The first principal component was extracted to integrate the normalized data of the four indicators. The weight values of each indicator were determined based on their contribution to the first principal component and their inherent characteristics, reducing errors associated with manual weight assignment. The models for each indicator are as follows:

2.3.1. Greenness—NDVI

The Normalized Difference Vegetation Index (NDVI), used for monitoring surface green vegetation cover, has become the most widely used vegetation index in remote sensing for monitoring green vegetation cover on the Earth's surface [33]. In this study, NDVI is utilized to represent greenness in the RSEI. The formula is as follows:

$$\mathrm{NDVI} = (\rho_{\mathrm{NIR}} - \rho_{\mathrm{red}}) / (\rho_{\mathrm{NIR}} + \rho_{\mathrm{red}}) \quad (1)$$

where the symbols and parameters are detailed in Table 1.

Table 1. Landsat satellite sensor parameters.

Satellite	Sensor Type	Band	Name	Wavelength Range (μm)	Central Wavelength (μm)
Landsat TM 5	Thematic Mapper (TM)	ρ_{blue}	Blue Band	0.450~0.520	0.4850
		ρ_{green}	Green Band	0.520~0.600	0.5600
		ρ_{red}	Red Band	0.630~0.690	0.6600
		ρ_{NIR}	Near-Infrared Band	0.760~0.900	0.8300
		ρ_{SWIR1}	Shortwave Infrared 1	1.550~1.750	1.6500
		ρ_{SWIR2}	Shortwave Infrared 2	10.400~12.500	11.4750
	Thermal Infrared Sensor (TIRS)	ρ_{TIRS1}	Thermal Infrared 1	2.080~2.350	2.2150
Landsat 8 OLI	Operational Land Imager (OLI)	ρ_{coastal}	Coastal Band	0.433~0.453	0.4430
		ρ_{blue}	Blue Band	0.450~0.515	0.4825
		ρ_{green}	Green Band	0.525~0.600	0.5625
		ρ_{red}	Red Band	0.630~0.680	0.6550
		ρ_{NIR}	Near-Infrared Band	0.845~0.885	0.8650
		ρ_{SWIR1}	Shortwave Infrared 1	1.560~1.660	1.6100
		ρ_{SWIR2}	Shortwave Infrared 2	2.100~2.300	2.2000
		ρ_{pan}	Panchromatic Band	0.500~0.680	0.6400
		ρ_{cirrus}	Cirrus Band	1.360~1.390	1.3750
	Thermal Infrared Sensor (TIRS)	ρ_{TIRS1}	Thermal Infrared 1	10.600~11.190	10.9000
		ρ_{TIRS2}	Thermal Infrared 2	11.500~12.510	12.0000

2.3.2. Wetness—WET

The wetness component (WET) is calculated using Tasseled Cap Transformation (also known as K-T transformation), which extracts parameters from Landsat image data. In this study, WET is used to represent the wetness in RSEI. However, due to differences in sensor parameters between Landsat TM 5 and Landsat OLI 8, the model parameters for WET differ accordingly [34,35]. The formula is as follows:

$$\mathrm{WET_{TM}} = \rho_{\mathrm{blue}} \times 0.0315 + \rho_{green} \times 0.2021 + \rho_{\mathrm{red}} \times 0.3102 + \rho_{\mathrm{NIR}} \times 0.1594 - \rho_{SWIR1} \times 0.6806 - \rho_{SWIR2} \times 0.6109 \quad (2)$$

$$\mathrm{WET_{OIL}} = \rho_{\mathrm{blue}} \times 0.1511 + \rho_{green} \times 0.1973 + \rho_{\mathrm{red}} \times 0.3283 + \rho_{\mathrm{NIR}} \times 0.3407 - \rho_{SWIR1} \times 0.7117 - \rho_{SWIR2} \times 0.4559 \quad (3)$$

where the symbols and parameters are detailed in Table 1.

2.3.3. Dryness—NDBSI

The Normalized Difference Bare Soil Index (NDBSI) is an effective metric for monitoring environmental dryness. It is calculated as the average of the Built-up Index (IBI) and the Bare Soil Index (SI) [36,37]. In this study, NDBSI is used to represent dryness in RSEI. The formula is as follows:

$$\mathrm{IBI} = \frac{\frac{2\rho_{SWIR1}}{\rho_{SWIR1}+\rho_{\mathrm{NIR}}} - \frac{\rho_{\mathrm{NIR}}}{\rho_{\mathrm{NIR}}+\rho_{\mathrm{red}}} - \frac{\rho_{green}}{\rho_{green}+\rho_{SWIR1}}}{\frac{2\rho_{SWIR1}}{\rho_{SWIR1}+\rho_{\mathrm{NIR}}} + \frac{\rho_{\mathrm{NIR}}}{\rho_{\mathrm{NIR}}+\rho_{\mathrm{red}}} + \frac{\rho_{green}}{\rho_{green}+\rho_{SWIR1}}} \quad (4)$$

$$\mathrm{SI} = \frac{(\rho_{SWIR1} + \rho_{\mathrm{red}}) - (\rho_{\mathrm{NIR}} + \rho_{\mathrm{blue}})}{(\rho_{SWIR1} + \rho_{\mathrm{red}}) + (\rho_{\mathrm{NIR}} + \rho_{\mathrm{blue}})} \quad (5)$$

$$\mathrm{NDBSI} = \frac{\mathrm{IBI} + \mathrm{SI}}{2} \quad (6)$$

where the symbols and parameters are detailed in Table 1.

2.3.4. Heat—LST

Land Surface Temperature (LST) was retrieved using the Radiative Transfer Equation (RTE) combined with Planck's law, based on Landsat thermal infrared imagery and atmospheric correction procedures. This method ensures accurate estimation of LST by accounting for surface emissivity, atmospheric effects, and sensor characteristics.

Surface emissivity (REf) was estimated using the Fractional Vegetation Cover (FVC) derived from NDVI values. Pixels were categorized into water, urban, and natural surfaces using NDVI thresholds. The emissivity values for different land surface types were assigned as follows: 0.995 for water, and polynomial expressions for building and natural surfaces as functions of FVC. The overall emissivity of each pixel was then calculated as a weighted average based on NDVI intervals (Equation (9)) [38,39].

The original digital number (DN) values from thermal bands were first converted to at-sensor radiance through radiometric calibration. Atmospheric correction was then applied using parameters including upward radiance (L_{up}), downward radiance (L_{down}), and atmospheric transmittance (t), The corrected surface-leaving radiance ($B(T_S)$) was calculated according to Equation (10), incorporating both emissivity and atmospheric effects.

$$\mathrm{FVC} = \mathrm{NDVI}_{<0.05} \times 0 + \mathrm{NDVI}_{>0.7} \times 1 + \mathrm{NDVI}_{0.05\sim0.7} \times \frac{\mathrm{NDVI}_{0.05\sim0.7} - 0.05}{0.7 - 0.05} \quad (7)$$

$$\begin{aligned} E(\mathrm{water}) &= 0.995 \\ E(\mathrm{building}) &= 0.9589 + 0.086 \times \mathrm{FVC} - 0.0671 \times \mathrm{FVC}^2 \\ E(\mathrm{natural}) &= 0.9625 + 0.0614 \times \mathrm{FVC} - 0.0461 \times \mathrm{FVC}^2 \end{aligned} \quad (8)$$

$$\mathrm{REf} = \mathrm{NDVI}_{\leq 0} \times E(\mathrm{water}) + \mathrm{NDVI}_{\leq 0\sim 0.7} \times E(\mathrm{building}) + \mathrm{NDVI}_{\geq 0.7} \times E(\mathrm{natural}) \quad (9)$$

$$B(TS) = \frac{\rho_{\mathrm{TIRS1}} - L_{\mathrm{up}} - t \times (1 - \mathrm{REf}) \times L_{\mathrm{down}}}{t \times \mathrm{REf}} \quad (10)$$

LST was computed using Planck's function, where the calibrated radiance values were transformed into brightness temperature values using the following equation:

$$\mathrm{LST} = \frac{K2}{\ln(\frac{K1}{B(TS)} + 1)} \tag{11}$$

where K1 and K2 are sensor-specific constants predefined by the satellite. For Landsat TM 5, K1 = 607.76 and K2 = 1260.56, while for Landsat 8 OLI-TIRS, K1 = 774.89 and K2 = 1321.08 [40,41]. Parameters are detailed in Table 1.

2.3.5. RSEI Model

By invoking the Principal Component Analysis (PCA) calculation model in GEE, the four factor indicators obtained above are coupled through PCA. The RSEI is constructed using the first principal component (PC 1). The greatest advantage of this approach is that the weights of the composite indicators are not manually assigned but are automatically and objectively determined based on the contribution of each indicator to PC 1. This avoids potential biases caused by subjective weight settings or methodological differences, thereby enhancing the objectivity and reliability of the results.

Since the dimensions of the four factors are uneven, directly using them for PCA calculation would result in unbalanced weights for each indicator. Therefore, before conducting PCA, the four factors should be normalized, converting each indicator value into a dimensionless range of 0~1 [42]. The formula is as follows:

$$\mathrm{XI}_i = \frac{I_i - I_{\min}}{I_{\max} - I_{\min}} \tag{12}$$

where $\mathrm{XI_i}$ is the normalized value, $\mathrm{I_i}$ is the original value before normalization, and $\mathrm{I_{max}}$ and $\mathrm{I_{min}}$ are the maximum and minimum values before normalization, respectively.

After the normalization of the four factors, there are cases where regions with better ecological conditions may have lower values. To address this, a positive-negative value transformation is applied, ensuring that higher RSEI values correspond to better ecological conditions. The formula is as follows:

$$\mathrm{RSEI} = 1 - \{\mathrm{PC1}[\mathrm{NDVI},\ \mathrm{WET},\ \mathrm{NDBSI},\ \mathrm{TEM}]\} \tag{13}$$

3. Results and Analysis

3.1. Spatiotemporal Analysis of Ecological Quality

Using OriginLab (Origin 2021, OriginLab Corporation, Northampton, MA, USA), the data for the four indicators and the RSEI were statistically analyzed and plotted as line charts. Based on the grading standards widely recognized by researchers, a classification system with a threshold of 0.2 was applied [43,44], dividing the RSEI into five levels: Excellent (0.8~1.0), Good (0.6~0.8), Moderate (0.4~0.6), Fair (0.2~0.4), and Poor (0.0~0.2).

As shown in Figure 2, the mean RSEI value of the STS from 2003 to 2023 is 0.390, corresponding to an overall ecological quality level of Fair. Over the 20-year period, RSEI exhibits a clear upward trend, increasing from 0.345 in 2003 to 0.447 in 2023 (an improvement of 29.59%), indicating a gradual recovery of ecological conditions. The increase is not uniform over time but shows more pronounced improvement after 2013, suggesting a transition from slow natural recovery to a relatively stable improving phase. The temporal variation in individual indicators reveals consistent patterns. NDVI shows a continuous increase from 0.398 to 0.453, reflecting sustained vegetation recovery. In contrast, WET exhibits relatively small interannual fluctuations and a slight overall decline, indicating limited changes in surface moisture conditions. LST shows a notable decreasing

trend, particularly after 2008, highlighting a gradual alleviation of surface thermal stress that is closely associated with increased vegetation cover and enhanced evapotranspiration. The NDBSI values display a general downward trend, implying reduced soil exposure and erosion intensity. The combined evolution of these indicators demonstrates that the long-term improvement in RSEI is mainly driven by vegetation recovery and surface cooling, while moisture conditions remain comparatively stable.

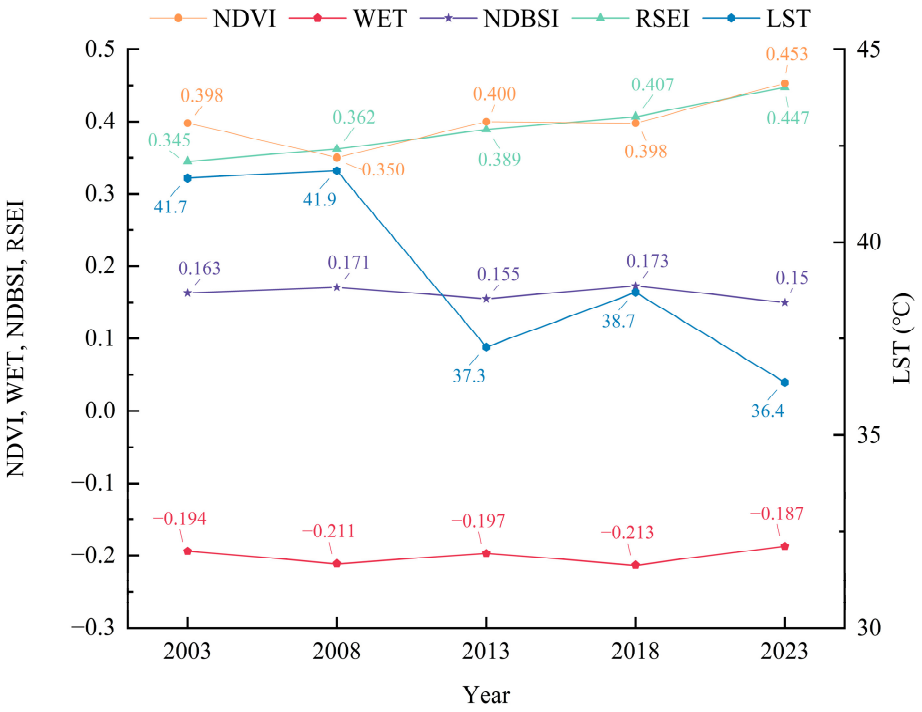


Figure 2. Temporal Distribution of NDVI, WET, NDBSI, RSEI, and LST at the STS from 2003 to 2023.

Using the aforementioned RSEI classification standards, the RSEI of the STS from 2003 to 2023 was reclassified using ArcGIS (version 10.5, Esri, Redlands, CA, USA), and ecological quality maps for the site were generated (Figure 3). The spatial distribution analysis reveals significant temporal and spatial variations in the ecological quality of the STS over the past 20 years. Higher ecological quality is consistently observed in the eastern part of the study area, particularly along river valley plains characterized by relatively fertile soils and better vegetation coverage. These areas predominantly fall into the Moderate or Good categories and exhibit relatively stable ecological conditions throughout the study period. In contrast, the western and northern regions, which are dominated by semi-arid landscapes with sparse vegetation, are largely classified as Fair or Moderate, indicating comparatively lower ecological quality. From a temporal perspective, the spatial patterns show a general improvement in ecological quality between 2003 and 2013, with noticeable expansion of Moderate and Good classes, especially in the eastern region. This improvement is accompanied by increased vegetation cover and reduced surface temperatures. Between 2013 and 2018, localized degradation is observed, particularly in parts of the western region, where ecological quality shifts toward lower classes. These changes spatially coincide with areas influenced by mining and industrial activities and may also reflect enhanced climatic stress during this period [45]. Since around 2018, enhanced ecological management and restoration initiatives, including drought-resistant vegetation planting and soil and water conservation projects, have been implemented in parts of the study area, as reported by international organizations [46]. After 2018, partial ecological recovery is evident in several western and northern areas, where regions previously classified as Fair transition back to Moderate by 2023. This recovery temporally overlaps

with reported ecological management and restoration initiatives, such as drought-resistant vegetation planting and soil and water conservation projects [45]. However, due to the absence of spatially explicit intervention data, these improvements cannot be quantitatively attributed to specific management measures. Throughout the entire period, the eastern region maintains relatively stable and higher ecological quality, supported by favorable natural conditions and gradual vegetation recovery. The observed spatial and temporal patterns highlight persistent contrasts between peripheral areas and the central test zone, indicating that while ecological conditions have generally improved, continued monitoring and targeted management remain necessary in the western and northern regions. Overall, the spatial and temporal variations in ecological quality at the STS reflect the effectiveness of the implemented restoration measures. However, the western and northern regions still require enhanced management and monitoring to further improve their ecological quality and recovery capacity.

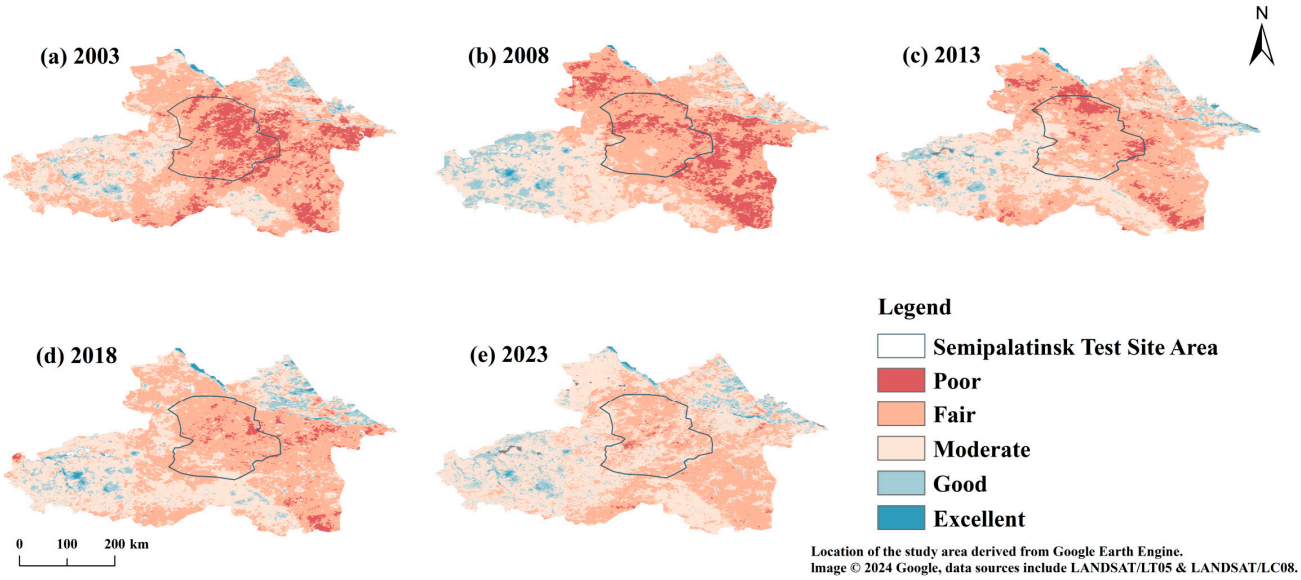


Figure 3. Ecological quality maps of the STS from 2003 to 2023.

Through ArcGIS, the area statistics for each RSEI grade from 2003 to 2023 were calculated, and the results are shown in Table 2. As seen in the table, the area of Poor-grade ecological quality decreased from 12,600 km^2 (14.99%) in 2003 to 500 km^2 (0.61%) in 2023. The Fair-grade area (low ecological quality) reduced from 43,600 km^2 (51.90%) in 2003 to 29,300 km^2 (34.92%) in 2023, indicating gradual improvement in these regions. The Moderate-grade area (medium ecological quality) increased significantly, rising from 24,400 km^2 (29.02%) in 2003 to 46,800 km^2 (55.76%) in 2023, becoming the dominant ecological quality grade. At the same time, the areas with Good and Excellent grades (higher and high-quality ecological conditions) grew from 3400 km^2 (4.04%) in 2003 to 7300 km^2 (8.87%) in 2023. Although the proportion of these grades increased more slowly, they still demonstrate a positive improvement trend. For the central nuclear test site, the ecological index has shifted from a widespread Poor grade in 2003 to Fair and Moderate grades in most areas by 2023, except for the Sary-Uzen test site, which remains in the Poor category. This is mainly due to the site's history of frequent underground nuclear tests, which left large amounts of radioactive nuclides in the soil [47]. These residual contaminants inhibit vegetation growth and cause significant changes in soil microbial community structures, further hindering ecological recovery. This situation reflects the need for longer recovery periods and more targeted remediation measures in the central nuclear test site area.

Table 2. Area statistics of ecological quality grades at the STS from 2003 to 2023.

Year	Poor		Fair		Moderate		Good		Excellent	
	Pct. %	Area/ 10^4 km^2	Pct. %	Area/ 10^4 km^2	Pct. %	Area/ 10^4 km^2	Pct. %	Area/ 10^4 km^2	Pct. %	Area/ 10^4 km^2
2003	14.99	1.26	51.90	4.36	29.02	2.44	3.73	0.31	0.36	0.03
2008	15.34	1.29	45.36	3.81	31.59	2.65	7.31	0.61	0.39	0.03
2013	6.49	0.55	48.58	4.08	39.23	3.30	5.24	0.44	0.45	0.04
2018	3.52	0.30	48.30	4.06	40.19	3.38	7.13	0.60	0.86	0.07
2023	0.61	0.05	34.92	2.93	55.76	4.68	8.18	0.69	0.53	0.04

3.2. Spatiotemporal Variation Analysis of Ecological Quality

Based on RSEI classification, to obtain dynamic information on ecological quality changes between different years, ArcGIS raster calculator was used to process RSEI for each year. The changes were categorized as Degraded (<0), No Change (=0), and Improved (>0). The results are presented in Table 3, with the spatial distribution shown in Figure 4.

Table 3. Proportions and areas of ecological quality changes in the STS from 2003 to 2023.

Classification	2003~2008		2008~2013		2013~2018		2018~2023		2003~2023	
	Pct. %	Area/ 10^4 km^2	Pct. %	Area/ 10^4 km^2	Pct. %	Area/ 10^4 km^2	Pct. %	Area/ 10^4 km^2	Pct. %	Area/ 10^4 km^2
Degraded	19.20	1.61	16.90	1.42	15.97	1.34	11.68	0.98	4.22	0.35
No Change	52.64	4.42	55.20	4.64	59.46	4.99	58.30	4.90	46.83	3.93
Improved	28.15	2.36	27.90	2.34	24.57	2.06	30.02	2.52	48.95	4.11

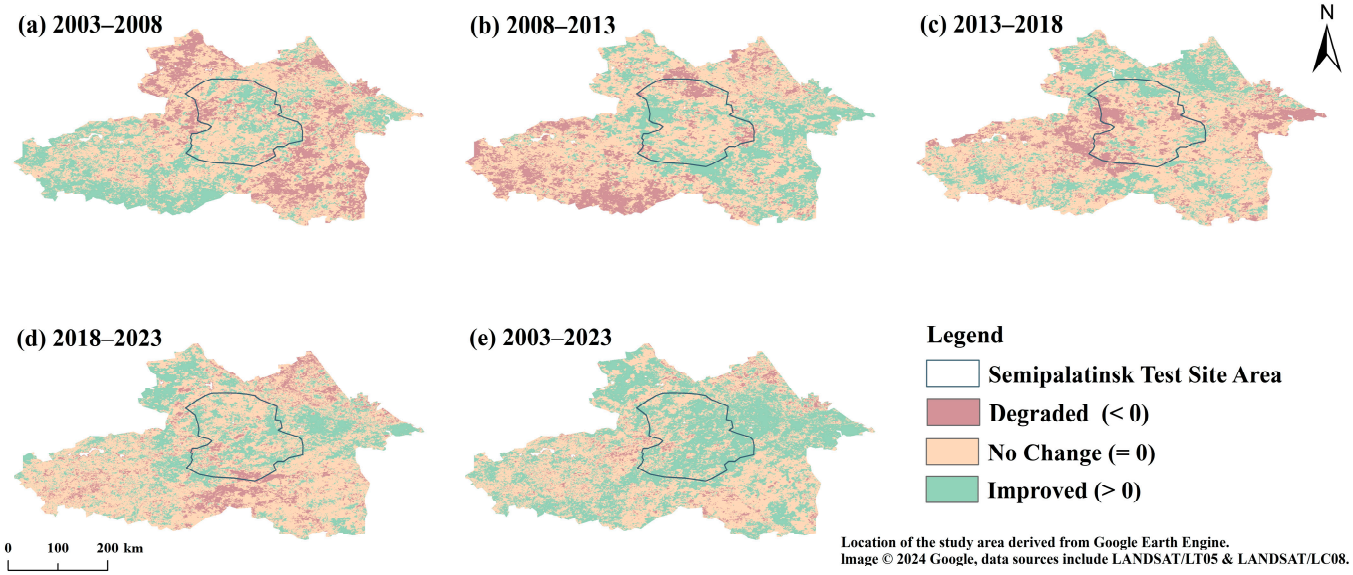


Figure 4. Spatiotemporal changes in ecological quality at the STS from 2003 to 2023.

The analysis of different phases from 2003 to 2023 shows that 2003–2008 was the phase with the highest proportion of degraded areas, accounting for 19.20% (16,100 km^2), while improved areas accounted for 28.15% (23,600 km^2). The degraded areas were mainly concentrated in the highly contaminated central test site, such as the Sary-Uzen test point. Studies indicate that this was due to the lack of natural recovery processes in the early restricted-access period, as well as the ineffective isolation of surface and subsurface radioactive contaminants. The surrounding areas exhibited low vegetation coverage, which provided limited recovery for soil structure and water bodies. 2008–2013, the proportion

of degraded areas decreased to 16.90% (14,200 km^2), while improved areas accounted for 27.90% (23,400 km^2). This phase's changes were closely related to the large-scale ecological restoration projects launched by the Kazakh government in 2008. Measures such as vegetation planting and isolating highly contaminated areas gradually reduced the migration of radioactive pollutants, improving the ecological quality of the surrounding regions. However, the core areas of the central test site still showed no significant improvement. 2013–2018, the proportion of degraded areas further declined to 15.97% (13,400 km^2), while unchanged areas increased to 59.46% (49,900 km^2), the highest proportion among all phases. During this period, the surrounding areas stabilized, indicating steady progress in ecological recovery. However, the core high-contamination areas (underground nuclear test zones) remained challenging to restore due to the persistent effects of deep-layer radioactive nuclides. 2018–2023, the proportion of improved areas reached 30.02% (25,200 km^2), the highest among all phases, while degraded areas dropped to 11.68% (9800 km^2). According to literature, the significant improvement during this phase was mainly attributed to further implementation of vegetation planting and soil and water conservation projects. Additionally, the surrounding areas experienced a significant increase in soil organic matter and vegetation coverage, resulting in notable ecological recovery.

From the overall trend between 2003 and 2023, improved areas accounted for a cumulative proportion of 48.95% (41,100 km^2), degraded areas for 19.88% (42,200 km^2), and unchanged areas for 46.83% (39,300 km^2). Improved areas were primarily distributed in the peripheral and river valley regions, where favorable natural conditions and minimal human intervention facilitated faster recovery. Although the ecological quality of the test site has shown significant improvement over the past 20 years, ecological restoration in highly contaminated areas remains challenging. Future remediation efforts should continue to focus on pollution isolation, deep soil restoration, and vegetation recovery, with particular emphasis on implementing targeted interventions for core contaminated areas to further promote comprehensive ecological recovery in the region.

3.3. PCA Results

The PCA results for the RSEI indicators across five selected years at the STS are shown in Table 4. The contribution rates of the first principal component (PC 1) for each year are 73.37%, 70.39%, 75.66%, 73.00%, and 74.57%, respectively, indicating that PC 1 captures the majority of the information from the four indicators and can be used to represent the overall ecological status of the study area. Over the 20-year period from 2003 to 2023, the contribution rates of PC 1 exhibit a relatively stable pattern, primarily driven by the long-term stability of temperature variation and vegetation cover. This suggests that the overall ecological characteristics of the region have remained comparatively stable during this period. Considering the characteristics of the region, this stability may reflect a gradual shift toward a relatively steady ecological state following the severe environmental impacts caused by nuclear testing.

The eigenvalues of NDVI and WET are positive, indicating their positive contributions to the ecological quality of the STS, whereas the eigenvalues of NDBSI and LST are negative, suggesting their adverse impacts on ecological conditions. The positive loadings of NDVI and WET in PC 1 imply that, despite the substantial initial ecological disturbances caused by nuclear testing, the ecosystem has experienced gradual recovery through natural vegetation regeneration and improved moisture conditions. In contrast, the negative influence of NDBSI and LST reflects the persistent effects of disrupted surface thermal balance and soil aridification associated with nuclear test activities. A comparison of the absolute eigenvalues of the four indicators across different years reveals a consistent order of influence: LST > NDVI > WET > NDBSI. This indicates that temperature is the most critical

factor affecting ecological quality in the region, likely related to long-term changes in surface physical properties and regional climate conditions following nuclear testing, while vegetation cover and moisture conditions act as secondary contributors and dryness plays a relatively minor role.

Table 4. Principal component analysis of indicators from 2000 to 2020.

Year	Eigenvalues	PC 1	PC 2	PC 3	PC 4
2003	NDVI	0.4550	−0.7869	0.4149	−0.0411
	LST	−0.8651	−0.5016	−0.0021	0.0061
	WET	0.2087	−0.3567	−0.9096	−0.0439
	NDBSI	−0.0332	0.0450	0.0229	−0.9982
	Contribution Rate/%	73.37	15.65	10.88	0.10
2008	NDVI	0.4134	−0.7099	0.5637	−0.0862
	LST	−0.8908	−0.4446	0.0940	0.0042
	WET	0.1814	−0.5375	−0.8206	−0.0697
	NDBSI	−0.0523	0.0974	0.0090	−0.9938
	Contribution Rate/%	70.39	16.60	11.17	1.84
2013	NDVI	0.4589	0.2117	0.8271	−0.2460
	LST	−0.7974	0.5123	0.3181	0.0226
	WET	0.2987	0.7660	−0.4611	−0.3337
	NDBSI	−0.2535	−0.3255	−0.0466	−0.9097
	Contribution Rate/%	75.66	12.76	9.55	2.03
2018	NDVI	0.5028	−0.5919	0.6298	−0.0169
	LST	−0.8346	−0.5221	0.1756	0.0013
	WET	0.2247	−0.6138	−0.7567	−0.0124
	NDBSI	−0.0123	0.0169	−0.0010	−0.9998
	Contribution Rate/%	73.00	14.86	10.91	1.23
2023	NDVI	0.5126	−0.4571	0.7244	−0.0595
	LST	−0.8110	−0.5352	0.2362	0.0007
	WET	0.2780	−0.7071	−0.6476	−0.0581
	NDBSI	−0.0474	0.0682	−0.0053	−0.9965
	Contribution Rate/%	74.57	14.35	9.75	1.33

To assess the robustness of the PCA-based RSEI construction, the temporal stability of the PCA structure was further examined. Across all selected years, PC 1 consistently explains more than 70% of the total variance, and the signs of the loadings for all four indicators remain unchanged, with NDVI and WET contributing positively, and LST and NDBSI contributing negatively. Moreover, the relative magnitude of the indicator loadings follows a stable pattern (LST > NDVI > WET > NDBSI) throughout the study period. This consistency demonstrates that the RSEI construction is structurally stable and not sensitive to interannual variations in data distribution, supporting the reliability of the PCA-based integration for long-term spatiotemporal ecological assessment.

4. Discussion

4.1. Spatiotemporal Characteristics of RSEI in Ecological Assessment of the Nuclear Test Site

This study applies the RSEI model to the STS for the first time, revealing the spatiotemporal evolution of ecological quality from 2003 to 2023. From a temporal perspective, the RSEI values show a significant overall improvement trend. During 2018–2023, the proportion of improved areas reached 30.02%, the highest in the 20-year period. This indicates that vegetation restoration and soil and water conservation measures implemented by the Kazakh government were highly effective in later stages. However, during 2003–2008, the proportion of degraded areas reached 19.20%, primarily concentrated in

highly contaminated areas in the early restricted-access period, such as the Sary-Uzen test point. This deterioration may be attributed to the ineffective containment of radioactive contaminants and the slow natural recovery process. From a spatial perspective, ecological recovery was more pronounced in peripheral areas, while significant delays were observed in the central region. The ecological quality in the central highly contaminated points has remained at poor levels over the long term, reflecting the persistent hindrance of deep-layer radioactive contamination on vegetation recovery and soil quality. The study results reveal a spatial distribution pattern of "peripheral improvement and central lag" in the ecological environment of the nuclear test site.

4.2. Driving Factors of Ecological Changes in the Nuclear Test Site

Ecological changes at the Semipalatinsk Test Site are controlled by the combined effects of climatic conditions, legacy nuclear contamination, and human activities. The PCA results indicate that land surface temperature (LST) exerts the strongest influence on ecological quality, reflecting the central role of surface thermal processes in this post-nuclear environment. Long-term radioactive contamination can indirectly modify soil structure and moisture retention, suppress microbial activity, and weaken evapotranspiration, leading to persistent surface heat accumulation. As a result, LST integrates both regional climatic variability and the long-term disturbance of soil–vegetation systems caused by nuclear testing.

Elevated surface temperatures further constrain ecosystem recovery by intensifying soil aridification, increasing vegetation water stress, and limiting plant physiological activity, thereby slowing vegetation succession and biomass accumulation. These thermal constraints help explain why temperature-related indicators dominate ecological variation in the STS, particularly in the semi-arid to temperate continental climate context. In contrast, peripheral areas benefit from relatively favorable environmental conditions and targeted restoration measures, while central zones remain ecologically constrained due to accumulated contamination and delayed soil–microbial recovery.

4.3. Global Significance of the RSEI Model in Nuclear Test Sites

The application of the RSEI model in this study provides a comprehensive and quantitative framework for assessing ecological recovery at nuclear test sites and offers broader insights for ecological monitoring in post-nuclear landscapes worldwide. Traditional evaluations of nuclear test sites often emphasize single factors, such as radionuclide distribution or vegetation cover change. In contrast, the RSEI framework integrates multiple surface ecological indicators, allowing for a holistic assessment of ecosystem responses under long-term contamination stress.

The "peripheral–center" recovery pattern identified at the Semipalatinsk Test Site (STS) is consistent with observations from other nuclear test sites, such as Bikini Atoll in the Marshall Islands and the Nevada Test Site (NTS) in the United States [48,49]. However, the underlying recovery mechanisms differ substantially across these sites due to contrasts in climatic conditions, ecosystem types, and dominant recovery drivers. At the Nevada Test Site, the arid desert climate, characterized by extremely low precipitation and sparse vegetation cover, severely constrains ecological recovery. Soil compaction, wind erosion, and limited biological productivity result in very slow revegetation, with estimated soil recovery times exceeding several centuries. In contrast, STS is located in a temperate continental to semi-arid climate zone, where seasonal precipitation and higher baseline vegetation coverage enable partial vegetation regeneration and soil moisture recovery, leading to more pronounced ecological improvements over time despite persistent contamination.

The comparison with Bikini Atoll further highlights the role of ecosystem type in shaping recovery trajectories. Bikini Atoll represents a marine ecosystem where ecological recovery is largely driven by hydrodynamic processes, larval dispersal, and coral recruitment, allowing for partial biological resilience even under severe radioactive disturbance [50]. In contrast, STS is a terrestrial ecosystem in which recovery is primarily governed by soil processes, vegetation succession, and land–atmosphere interactions. These processes are inherently slower and more sensitive to long-term radionuclide contamination, particularly in core test areas. Importantly, STS also differs from Bikini Atoll in that it remains partially accessible to human intervention, making active ecological restoration and management measures more feasible.

Together, these comparisons suggest that while the "peripheral–center" pattern may represent a common spatial response to nuclear disturbance, the pace and pathways of ecological recovery are strongly modulated by climate regime, ecosystem type, and the relative roles of natural versus human-driven recovery processes. This conceptual distinction provides a more general framework for understanding post-nuclear ecological recovery across diverse environmental settings and supports the broader applicability of integrated remote sensing–based indices such as RSEI in comparative nuclear site assessments.

The application of the RSEI model to nuclear test sites represents an exploratory yet transferable approach for standardized ecological assessment in highly contaminated environments. While the RSEI framework effectively captures integrated surface ecological responses, it does not explicitly incorporate radionuclide-related processes that fundamentally constrain ecosystem recovery in core contaminated zones. In this study, the persistent low ecological quality observed in central areas is indirectly reflected through suppressed vegetation growth, altered moisture conditions, and disrupted surface thermal regimes. The integration of remote sensing technology and ecological indices such as RSEI addresses key challenges in monitoring nuclear test sites where field surveys are constrained by safety concerns, demonstrating the model's global applicability for long-term ecological assessment. In regions characterized by limited field accessibility or high contamination risks, remote sensing–based ecological indices provide a practical tool to support environmental governance, ecological restoration planning, and sustainable development in post-nuclear landscapes.

4.4. Limitations and Recommendations for Ecological Governance

Despite the effectiveness of the RSEI model in assessing ecological changes at the STS, several limitations should be acknowledged. This study relies primarily on remote sensing data and lacks field-based validation, which may limit the representation of complex processes such as groundwater contamination, microbial dynamics, and soil nutrient conditions. In addition, due to constraints in data availability and climatic conditions affecting satellite observations, a five-year interval was adopted, which may not capture short-term ecological fluctuations or extreme events. The applicability of the RSEI model in strongly radioactive contaminated areas should be interpreted with caution, as radiation-induced alterations in vegetation physiology and soil properties may influence spectral responses that are not explicitly accounted for in the model. Since the Semipalatinsk Test Site has been officially closed and access to highly contaminated zones is strictly restricted, direct ground-truth verification using field eco-logical data is currently not feasible.

In addition, the use of the Google Earth Engine platform introduces certain methodological uncertainties. Although cloud and cloud-shadow masking and seasonal compositing were applied, residual cloud contamination may still remain in some areas. Furthermore, sensor calibration differences between Landsat missions and algorithmic artifacts associated with large-scale compositing and mosaicking procedures may influence local-

scale variability. These uncertainties are inherent to long-term, large-area satellite-based analyses and should be considered when interpreting fine-scale spatial variations, although they are unlikely to alter the overall spatial patterns and temporal trends identified in this study.

To improve ecological assessment and governance of nuclear test sites, several recommendations can be proposed. For heavily contaminated zones, multi-level restoration strategies—including soil remediation, contaminant isolation, and vegetation recovery—should be prioritized. These restoration measures are discussed at a conceptual level, and their specific technical implementation should be determined through site-specific engineering and radiological risk assessments. The RSEI model, particularly when combined with high-resolution remote sensing data, can serve as an effective tool for dynamic monitoring and long-term ecological evaluation in regions where field surveys are limited by safety constraints. Future research should focus on improving the validation and applicability of RSEI by integrating high-resolution remote sensing, UAV-based imagery, and field investigations when safety conditions permit. Strengthening international cooperation and the sharing of technical expertise would further support standardized assessment frameworks, evidence-based policy development, and transferable ecological restoration strategies for similarly impacted regions worldwide.

5. Conclusions

This study was designed to evaluate the long-term spatiotemporal evolution of ecological quality at the Semipalatinsk Test Site using the RSEI framework, identify its dominant driving factors, and explore its applicability for ecological governance in nuclear-contaminated environments. This study systematically evaluated the ecological quality of the STS from 2003 to 2023 using the RSEI model, revealing spatiotemporal characteristics and driving factors of ecological recovery. The results showed a significant improvement in the RSEI, increasing from 0.345 in 2003 to 0.447 in 2023, a rise of 29.59%. The area of "Poor" quality decreased dramatically from 14.99% in 2003 to 0.61% in 2023, while "Moderate" and "Good" quality areas rose from 29.02% and 4.04% to 55.76% and 8.87%, respectively, reflecting an overall trend of ecological recovery. Peripheral areas showed significant improvement due to favorable natural conditions and effective management measures, while highly polluted areas, such as the Sary-Uzen test site, lagged due to persistent contamination and soil degradation.

Principal component analysis indicated that temperature (LST) had the greatest impact on ecological quality, followed by vegetation (NDVI) and wetness (WET). Temperature changes were identified as a critical driver of ecological recovery, as radioactive contamination disrupted the surface thermal balance. While improvements in vegetation and humidity enhanced some areas, long-term pollution and residual issues from underground nuclear testing continued to hinder recovery in highly contaminated regions.

The period from 2003 to 2008 had the highest proportion of degraded areas (19.20%) due to the site's closure and lack of ecological restoration efforts. From 2018 to 2023, the proportion of improved areas reached 30.02%, demonstrating the effectiveness of later-stage measures such as vegetation restoration and soil conservation. These spatiotemporal differences further confirmed the "peripheral–core" effect of nuclear testing, where peripheral areas recover faster due to advantageous conditions, while core areas recover more slowly due to accumulated contamination and higher restoration challenges.

This study represents the first application of the RSEI model to the long-term ecological assessment of a nuclear test site, providing a quantitative analysis of spatiotemporal ecological changes and key driving factors at the Semipalatinsk Test Site over the past two decades. By integrating multiple surface ecological indicators, the RSEI framework captures

recovery patterns, dominant thermal constraints, and the persistent "peripheral–center" spatial differentiation associated with legacy nuclear contamination. These findings directly address the objectives of this study and offer practical insights for ecological monitoring and management of nuclear test sites, highlighting the importance of targeted strategies such as contamination isolation, soil restoration, and vegetation recovery in core contaminated zones. Future research should further enhance the applicability of RSEI-based assessments through the integration of high-resolution remote sensing data, UAV observations, and field investigations where safety conditions permit, supporting more effective ecological restoration and sustainable management of post-nuclear landscapes.

Supplementary Materials: The following supporting information can be downloaded at: https://www.mdpi.com/article/10.3390/su18010206/s1, landsat5-RSEI-Code; landsat8-RSEI-Code.

Author Contributions: Conceptualization, M.C. and N.K.; methodology, A.S. and M.C.; software, A.S.; validation, A.S., V.B.V. and M.C.; formal analysis, A.S.; investigation, A.S.; resources, N.K.; data curation, A.S.; writing—original draft preparation, A.S.; writing—review and editing, M.C., N.K. and V.B.V.; visualization, A.S.; supervision, M.C. and N.K.; project administration, M.C.; funding acquisition, A.S. All authors have read and agreed to the published version of the manuscript.

Funding: This work was supported by Japan Science and Technology Agency: JPMJSP2132.

Institutional Review Board Statement: Not applicable.

Informed Consent Statement: Not applicable.

Data Availability Statement: The original contributions presented in this study are included in the article/Supplementary Materials. Further inquiries can be directed to the corresponding author.

Acknowledgments: The authors sincerely thank the editors and anonymous reviewers for their kind view and constructive suggestions.

Conflicts of Interest: The authors declare no conflicts of interest.

References

1. Genay, L. The First Atomic Bomb: The Trinity Site in New Mexico. *Pac. Hist. Rev.* **2024**, *93*, 158–160. [CrossRef]
2. Pravalie, R. Nuclear Weapons Tests and Environmental Consequences: A Global Perspective. *Ambio* **2014**, *43*, 729–744. [CrossRef] [PubMed]
3. Stawkowski, M.E. "I am a radioactive mutant": Emergent biological subjectivities at Kazakhstan's Semipalatinsk Nuclear Test Site. *Am. Ethnol.* **2016**, *43*, 144–157. [CrossRef]
4. Bouville, A. Fallout from Nuclear Weapons Tests: Environmental, Health, Political, and Sociological Considerations. *Health Phys.* **2020**, *118*, 360–381. [CrossRef]
5. Chaizhunusova, N.; Madiyeva, M.; Tanaka, K.; Hoshi, M.; Kawano, N.; Noso, Y.; Takeichi, N.; Rakhypbekov, T.; Urazalina, N.; Dovgal, G.; et al. Cytogenetic abnormalities of the descendants of permanent residents of heavily contaminated East Kazakhstan. *Radiat. Environ. Biophys.* **2017**, *56*, 337–343. [CrossRef]
6. Zheng, J.M.; Long, B.; Xie, F.Y. General mechanisms for policy-making on environmental remediation at the post-closure nuclear test sites in the USA. *Environ. Sci. Pollut. Res.* **2020**, *27*, 11484–11493. [CrossRef]
7. Jayaprakash, N.D. Nuclear disarmament and India. *Econ. Polit. Wkly.* **2000**, *35*, 525–533.
8. Ringbom, A.; Axelsson, A.; Aldener, M.; Auer, M.; Bowyer, T.W.; Fritioff, T.; Hoffman, I.; Khrustalev, K.; Nikkinen, M.; Popov, V.; et al. Radioxenon detections in the CTBT international monitoring system likely related to the announced nuclear test in North Korea on February 12, 2013. *J. Environ. Radioact.* **2014**, *128*, 47–63. [CrossRef]
9. Lu, Y.L.; Yuan, J.J.; Du, D.; Sun, B.; Yi, X.J. Monitoring long-term ecological impacts from release of Fukushima radiation water into ocean. *Geogr. Sustain.* **2021**, *2*, 95–98. [CrossRef]
10. Zhang, X.R.; Wang, Z.B.; Lin, J. GIS Based Measurement and Regulatory Zoning of Urban Ecological Vulnerability. *Sustainability* **2015**, *7*, 9924–9942. [CrossRef]
11. Zhou, Q.W.; He, Y.; Wu, H.Y.; Li, Y.Q. Environmental carrying capacity of green resource city ecological landscape supported by GIS. *Int. J. Environ. Technol. Manag.* **2022**, *25*, 519–543. [CrossRef]

12. Chen, M.W.; Wang, T.X.; Liu, Y.Q.; Zhang, S.K.; Zhang, Y. Research on remote sensing ecological livability index based on Google Earth Engine: A case study from UrumqiChangji-Shihezi urban cluster. *PeerJ* **2024**, *12*, 23. [CrossRef] [PubMed]
13. Xiong, Y.; Xu, W.H.; Lu, N.; Huang, S.D.; Wu, C.; Wang, L.G.; Dai, F.; Kou, W.L. Assessment of spatial–temporal changes of ecological environment quality based on RSEI and GEE: A case study in Erhai Lake Basin, Yunnan province, China. *Ecol. Indic.* **2021**, *125*, 10. [CrossRef]
14. Huang, H.P.; Chen, W.; Zhang, Y.; Qiao, L.; Du, Y.Y. Analysis of ecological quality in Lhasa Metropolitan Area during 1990-2017 based on remote sensing and Google Earth Engine platform. *J. Geogr. Sci.* **2021**, *31*, 265–280. [CrossRef]
15. Ma, D.L.; Huang, Q.J.; Liu, B.Z.; Zhang, Q. Analysis and Dynamic Evaluation of Eco-Environmental Quality in the Yellow River Delta from 2000 to 2020. *Sustainability* **2023**, *15*, 7835. [CrossRef]
16. Amiri, F.; Jamali, A.A.; Gharibvand, L.K. Tracing air pollution changes (CO, NO2, SO2, and HCHO) using GEE and Sentinel 5P images in Ahvaz, Iran. *Environ. Monit. Assess.* **2023**, *195*, 12. [CrossRef]
17. Boori, M.S.; Choudhary, K.; Paringer, R.; Kupriyanov, A. Eco-environmental quality assessment based on pressure-state-response framework by remote sensing and GIS. *Remote Sens. Appl. Soc. Environ.* **2021**, *23*, 19. [CrossRef]
18. Cheng, H.R.; Zhu, L.K.; Meng, J.J. Fuzzy evaluation of the ecological security of land resources in mainland China based on the Pressure-State-Response framework. *Sci. Total Environ.* **2022**, *804*, 14. [CrossRef]
19. Das, S.; Bhunia, G.S.; Bera, B.; Shit, P.K. Evaluation of wetland ecosystem health using geospatial technology: Evidence from the lower Gangetic flood plain in India. *Environ. Sci. Pollut. Res.* **2022**, *29*, 1858–1874. [CrossRef]
20. Hu, X.S.; Xu, H.Q. A new remote sensing index for assessing the spatial heterogeneity in urban ecological quality: A case from Fuzhou City, China. *Ecol. Indic.* **2018**, *89*, 11–21. [CrossRef]
21. Xu, H.Q.; Duan, W.F.; Deng, W.H.; Lin, M.J. RSEI or MRSEI? Comment on Jia et al. Evaluation of Eco-Environmental Quality in Qaidam Basin Based on the Ecological Index (MRSEI) and GEE. *Remote Sens.* **2021**, *13*, 4543. *Remote Sens.* **2022**, *14*, 5307. [CrossRef]
22. Xu, H.Q.; Wang, M.Y.; Shi, T.T.; Guan, H.D.; Fang, C.Y.; Lin, Z.L. Prediction of ecological effects of potential population and impervious surface increases using a remote sensing based ecological index (RSEI). *Ecol. Indic.* **2018**, *93*, 730–740. [CrossRef]
23. Kamran, M.; Yamamoto, K. Analysis and visualization of spatio-temporal variations of ecological vulnerability in Pakistan using satellite observation datasets. *Environ. Sustain. Indic.* **2024**, *23*, 17. [CrossRef]
24. Liu, C.L.; Li, Y.W.; He, D.M.; Deng, B.W.; Zhang, E.W.; Wei, S.Z.; Duan, X.W. Dynamic monitoring of eco-environmental quality in the Greater Mekong Subregion: Evolutionary characteristics and country differences. *Environ. Impact Assess. Rev.* **2025**, *110*, 15. [CrossRef]
25. Ye, B.W.; Sun, B.; Shi, X.H.; Zhao, Y.L.; Guo, Y.Y.; Pang, J.Q.; Yao, W.Z.; Hu, Y.X.; Zhao, Y.X. Monitoring and Analysis of Eco-Environmental Quality in Daihai Lake Basin from 1985 to 2022 Based on the Remote Sensing Ecological Index. *Sustainability* **2024**, *16*, 6854. [CrossRef]
26. Aidarkhanova, A.; Larionova, N.; Tashekova, A.; Dyussembayeva, M.; Mamyrbayeva, A.; Timonova, L.; Shakenov, Y.; Mulikova, A.; Aidarkhanov, A. Assessment of the radionuclide and chemical composition of the Irtysh River water at the Republic of Kazakhstan territory. *RSC Adv.* **2024**, *14*, 26208–26218. [CrossRef]
27. Kawano, N.; Ohtaki, M. Remarkable experiences of the nuclear tests in residents near the Semipalatinsk Nuclear Test Site: Analysis based on the questionnaire surveys. *J. Radiat. Res.* **2006**, *47*, A199–A207. [CrossRef]
28. Yankauskas, A.; Larionova, N.; Shatrov, A.; Toporova, A. The Effect of Radionuclide and Chemical Contamination on Morphological and Anatomical Parameters of Plants. *Plants* **2024**, *13*, 2860. [CrossRef]
29. Aitenova, A.; Kulsariyeva, A.; Ryskieva, A. "Struggle for Peace, in their Own Land" as the Philosophy of the "Nevada-Semipalatinsk" Movement. *Hum. Aff.* **2024**, *34*, 106–118. [CrossRef]
30. Nurpeisova, M.; Bekbassarov, S.; Umirbayeva, A.; Kyrgizbaeva, D.; Madimarova, G.; Kapassova, A. Ecological Mapping of the Territory on the Basis of Integrated Monitoring. *Biosci. Biotechnol. Res. Commun.* **2019**, *12*, 55–66.
31. Semenova, Y.; Pivina, L.; Manatova, A.; Bjorklund, G.; Glushkova, N.; Belikhina, T.; Dauletyarova, M.; Zhunussova, T. Mental distress in the rural Kazakhstani population exposed and non-exposed to radiation from the Semipalatinsk Nuclear Test Site. *J. Environ. Radioact.* **2019**, *203*, 39–47. [CrossRef] [PubMed]
32. Sultangazin, U. Information systems based on space monitoring for solution of some problems of sustainable development. *Math. Comput. Simul.* **2004**, *67*, 279–290. [CrossRef]
33. Rouse, J.W.; Haas, R.H.; Schell, J.A.; Deering, D.W. Monitoring vegetation systems in the Great Plains with ERTS. *NASA Spec. Publ.* **1974**, *351*, 309.
34. Baig, M.H.A.; Zhang, L.F.; Shuai, T.; Tong, Q.X. Derivation of a tasselled cap transformation based on Landsat 8 at-satellite reflectance. *Remote Sens. Lett.* **2014**, *5*, 423–431. [CrossRef]
35. Crist, E.P.; Laurin, R.; Colwell, J.E.; Kauth, R.J. *Investigations of Vegetation and Soils Information Contained in Landsat Thematic Mapper and Multispectral Scanner Data*; NASA: Washington, DC, USA, 1984; pp. 301–306.

36. Essa, W.; Verbeiren, B.; van der Kwast, J.; Van de Voorde, T.; Batelaan, O. Evaluation of the DisTrad thermal sharpening methodology for urban areas. *Int. J. Appl. Earth Obs. Geoinf.* **2012**, *19*, 163–172. [CrossRef]
37. Xu, H. A new index for delineating built-up land features in satellite imagery. *Int. J. Remote Sens.* **2008**, *29*, 4269–4276. [CrossRef]
38. Jiménez-Muñoz, J.C.; Cristóbal, J.; Sobrino, J.A.; Sória, G.; Ninyerola, M.; Pons, X. Revision of the Single-Channel Algorithm for Land Surface Temperature Retrieval From Landsat Thermal-Infrared Data. *IEEE Trans. Geosci. Remote Sens.* **2009**, *47*, 339–349. [CrossRef]
39. Nichol, J. Remote sensing of urban heat islands by day and night. *Photogramm. Eng. Remote Sens.* **2005**, *71*, 613–621. [CrossRef]
40. Sobrino, J.A.; Jiménez-Muñoz, J.C.; Paolini, L. Land surface temperature retrieval from LANDSAT TM 5. *Remote Sens. Environ.* **2004**, *90*, 434–440. [CrossRef]
41. Weng, Q.H. Thermal infrared remote sensing for urban climate and environmental studies: Methods, applications, and trends. *ISPRS-J. Photogramm. Remote Sens.* **2009**, *64*, 335–344. [CrossRef]
42. Amani, M.; Ghorbanian, A.; Ahmadi, S.A.; Kakooei, M.; Moghimi, A.; Mirmazloumi, S.M.; Moghaddam, S.H.A.; Mahdavi, S.; Ghahremanloo, M.; Parsian, S.; et al. Google Earth Engine Cloud Computing Platform for Remote Sensing Big Data Applications: A Comprehensive Review. *IEEE J. Sel. Top. Appl. Earth Observ. Remote Sens.* **2020**, *13*, 5326–5350. [CrossRef]
43. Pan, W.H.; Wang, S.Y.; Wang, Y.; Yu, Y.J.; Luo, Y.Y. Dynamical changes of land use/land cover and their impacts on ecological quality during China's reform periods: A case study of Quanzhou city, China. *PLoS ONE* **2022**, *17*, 27. [CrossRef]
44. Zhang, J.; Zheng, S.L.; Sun, Y.; Yue, H.J. Landscape ecological risk assessment of an ecological area in the Kubuqi desert based on Landsat remote sensing data. *PLoS ONE* **2023**, *18*, 20. [CrossRef]
45. Salnikov, V.; Turulina, G.; Polyakova, S.; Petrova, Y.; Skakova, A. Climate change in Kazakhstan during the past 70 years. *Quat. Int.* **2015**, *358*, 77–82. [CrossRef]
46. Programme, U.N.D. The UN Development Programme Presented the Outcomes of the Large-Scale Initiative on Biodiversity Conservation and Forest Restoration in Kazakhstan. Available online: https://www.undp.org/kazakhstan/press-releases/un-development-programme-presented-outcomes-large-scale-initiative-biodiversity-conservation-and-forest-restoration (accessed on 17 October 2025).
47. Krivitskiy, P.Y.; Larionova, N.V.; Monayenko, V.N.; Subbotin, S.B.; Chernov, A.A.; Panitskiy, A.V. Peculiarities of radioactive soil contamination in places of underground nuclear tests in the Semipalatinsk test site. *J. Environ. Radioact.* **2022**, *253–254*, 106991. [CrossRef] [PubMed]
48. Richards, Z.T.; Beger, M.; Pinca, S.; Wallace, C.C. Bikini Atoll coral biodiversity resilience five decades after nuclear testing. *Mar. Pollut. Bull.* **2008**, *56*, 503–515. [CrossRef]
49. Webb, R.H.; Wilshire, H.G. Recovery of soils and vegetation in a Mojave desert ghost town, Nevada, U.S.A. *J. Arid. Environ.* **1980**, *3*, 291–303. [CrossRef]
50. Masami, N.; Masakazu, H.; Yoshinori, H.; Shinjiro, S. Bikini: 50 Years of Nuclear Exposure. *Asia-Pac. J.* **2004**, *2*, e5. [CrossRef]

Disclaimer/Publisher's Note: The statements, opinions and data contained in all publications are solely those of the individual author(s) and contributor(s) and not of MDPI and/or the editor(s). MDPI and/or the editor(s) disclaim responsibility for any injury to people or property resulting from any ideas, methods, instructions or products referred to in the content.